Chapter 7 Delamination Analysis of Skin-stiffener

7.1 Introduction

In the present chapter strain energy release rate as a fracture parameter has been used to evaluate the skin-stiffener debonding in stiffened composite panel with functionally-graded (FG) bimodular material property under thermo-mechanical coupled field. The influence of ply lay-up and interaction of residual thermal stresses on the skin-stiffener has been investigated. Stress dependent elasticity problem of bimodular stiffened panel made up of laminated Fiber Reinforced Polymeric (FRP) composite is carried out using Finite Element Analysis under various bimodular ratios. The numerical result in terms of compressive load as a function of applied displacement has been compared to the existing literature data to assess the effectiveness of the implemented methodology. Variation of energy release rate along the interface delamination front has been plotted for both mechanical and thermo-mechanical coupled loading with bimodulus ratio R varying from 1 (unimodular) to 5. Asymmetric variation of energy release rate along the interfacial front has been observed for the bimodular stiffened composite panel. It has been found that the bimodularity significantly reduces the failure growth. In retrospect, involvement of residual thermal stresses and bimodularity on fracture behavior of stiffened composite panels containing pre-existing embedded delaminations has been the impetus of the present study. In real structures these embedded delaminations are of very small dimension to be detected by existing non-destructive techniques for detecting flaws. Laboratory scale experimentation of inserting teflon sheets between adjacent plies for replicating such delamination behavior fail to address this delamination progression behavior properly.

7.2 Numerical analysis

The numerical methodology introduced in preceding section has been applied to determine the strain energy release rate of skin-stiffener with functionally graded bimodularity under thermo-mechanical loading. A literature [162] test case, consisting of a single-stiffener composite panel with an artificial skin-stiffener debonding. In this section the description of test case is provided along with the numerical results obtained from the Finite Element Method (FEM). The result is evaluated and compared with literature simulated data, in terms of load versus applied displacement curve.

7.2.1 A numerical approach for delamination

This methodology is able to overcome the drawbacks related to standard VCCT-fail release approach. This proposed numerical approach is the combination of three separated and interacting mechanisms [82]. The first mechanism “SMART-TIME” is an iterative procedure in which suitably changing load step size gives the element length along the delamination front, thus delamination growth dependence on the finite elements size and the load-step size is avoided.

The second mechanism is based on the modification of the algorithm proposed by Xie and Bigger [182,183] aimed to determine the correct local coordinates system and the correct virtually released area associated to each node on the delamination front regardless of delamination front shape and smoothness. This approach is named as “XB”. This method is able to determine the local coordinates system orientation from the instantaneous shape of the delamination front at each node, thus energy release rate components is computed.

The third mechanism is implemented to solve the problem of uncorrected peaks in the SERR distribution that appear at corner nodes of non-smooth delamination fronts. These

peaks are because of the nodal fail release approach itself, even when the XB approach is used to evaluate the correct energy release rate components and the correct released area for each node on the delamination front.

The combination of described three mechanisms has been found very effective for circular delamination growth but not found suitable for the simulation of skin-stiffener debonding inter-laminar defects evolution. So, the definition of delamination boundaries has been improved by modifying XB module. This numerical approach is named as "SMart time XB approach for Skin Stringer debonding" or "SMXB-SS". In this paper, skin-stiffener debonding with FG bimodular material properties is evaluated and verified by this mechanism.

7.2.2 Test-case description and FEM model

The Finite Element model of a stiffened panel and the numerical approach for the simulation of inter-laminar damage has been implemented in the ANSYS code using APDL. The modified subroutine is used to evaluate the failure of stiffener under thermal residual effect with FG bimodular material properties.

The geometry of the skin-stiffener panel is shown in Figure 7.1. The material properties of the graphite/epoxy are mentioned in Table 7.1. The stiffened panel is debonded at the middle of structure and edges have been enclosed in potting to ensure uniform distribution of the applied load (refer Figure 7.1). The composite laminate characteristics for the analyzed configuration are reported in Table 7.2. Material of the skin-stiffener is graded with functionally graded bimodularity. It is implemented through continuous variation of elastic modulus which is governed by linear function profile (Equation 3.15). The skin-stiffener is made of FG whose properties vary from material 1 to material 2. Material properties measured in terms of bimodulus ratio 'R' which varies from 1 to 5. The upper

bound modulus E_T is taken as values given in Table 7.1 and lower bound modulus E_C is varied according to bimodulus ratio 'R' as expressed in Equation (3.17). The Poisson's ratio for tension is considered as values given in Table 7.1 and Poisson's ratio for compression ν_C can be calculated with the help of relation defined in Equation (3.19). Tension and compression parts of the panel have been modeled separately according to the Equation 5.1.

The skin, flange and stiffener have been modeled using higher order 3-D 20-node solid layered element that exhibits quadratic displacement behavior having three degrees of freedom per node: translations in the nodal x, y, and z directions in ANSYS 14.5. A three-dimensional meshing pattern of the panel is shown in Figure 7.2. Mesh refinement has been done at the critical area where cracking is observed during the test. Figure shows that the view of finite element (FE) model developed for studying the thermo-elastic effect on fracture crack growth behavior of embedded graphite/epoxy laminate specimen.

The contact element has been placed in the debonded region of the panel to avoid penetration between the components and in the non-debonded area, skin and stiffener have been connected by contact elements with birth and death capabilities to allow separation when the growth criterion satisfied (Fig 7.3). It is clear from figure that one edge of the stiffened panel has been clamped while on other, compressive displacement has been applied in case of mechanical loading. For studying the thermo-elastic stress behavior, axial loading is applied subsequent to the uniform temperature drop from stress free state at 300^0 C to the 30^0 C room temperature to induce thermal residual stresses in the stiffener. In the potting section, only lateral and out of plane displacements have been constrained.

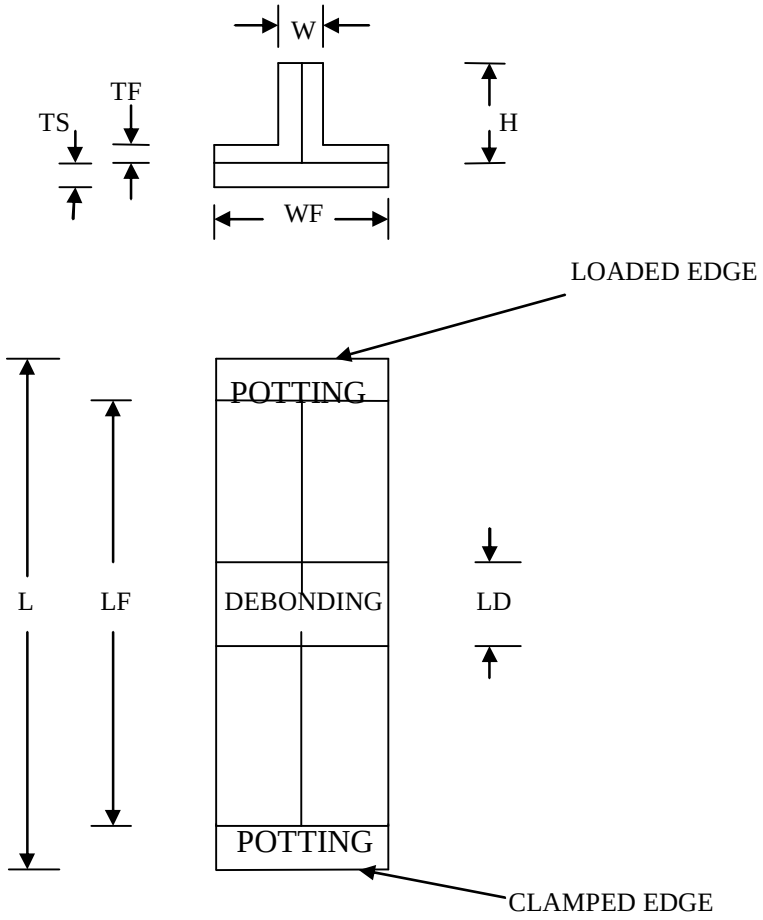

PARAMETERS	VALUES (mm)
W	3
TS	1
TF	1.5
H	14
WF	32
LF	300
LD	80
L	400

Figure 7.1 Geometrical description of the stiffened panel

Table 7.1 Material Properties of graphite/epoxy [82]

Stiffness property	Value
E_{11}	147000 MPa
$E_{22} = E_{33}$	11800 MPa
$G_{12} = G_{13}$	6000 MPa
G_{23}	4000 MPa
$\nu_{12} = \nu_{13}$	0.3
ν_{23}	0.4
$\alpha_x = \alpha_y$	0.025e-6 /^{o}C
α_z	22.5e-6 /^{o}C

Temperature state:
Curing temperature = 300^{o}C
Room temperature = 30^o
ΔT = -270^{o}C

Table 7.2 Composite Laminate Parameters

PARAMETER	CONFIGURATION
SKIN LAY-UP	$[90,+45,-45,0]_S$
FLANGE LAY-UP	$[(+45,-45)_3,O_6]$
STIFFENER LAY-UP	$[(+45,-45)_3,O_6]_S$
PLY THICKNESS	0.125mm

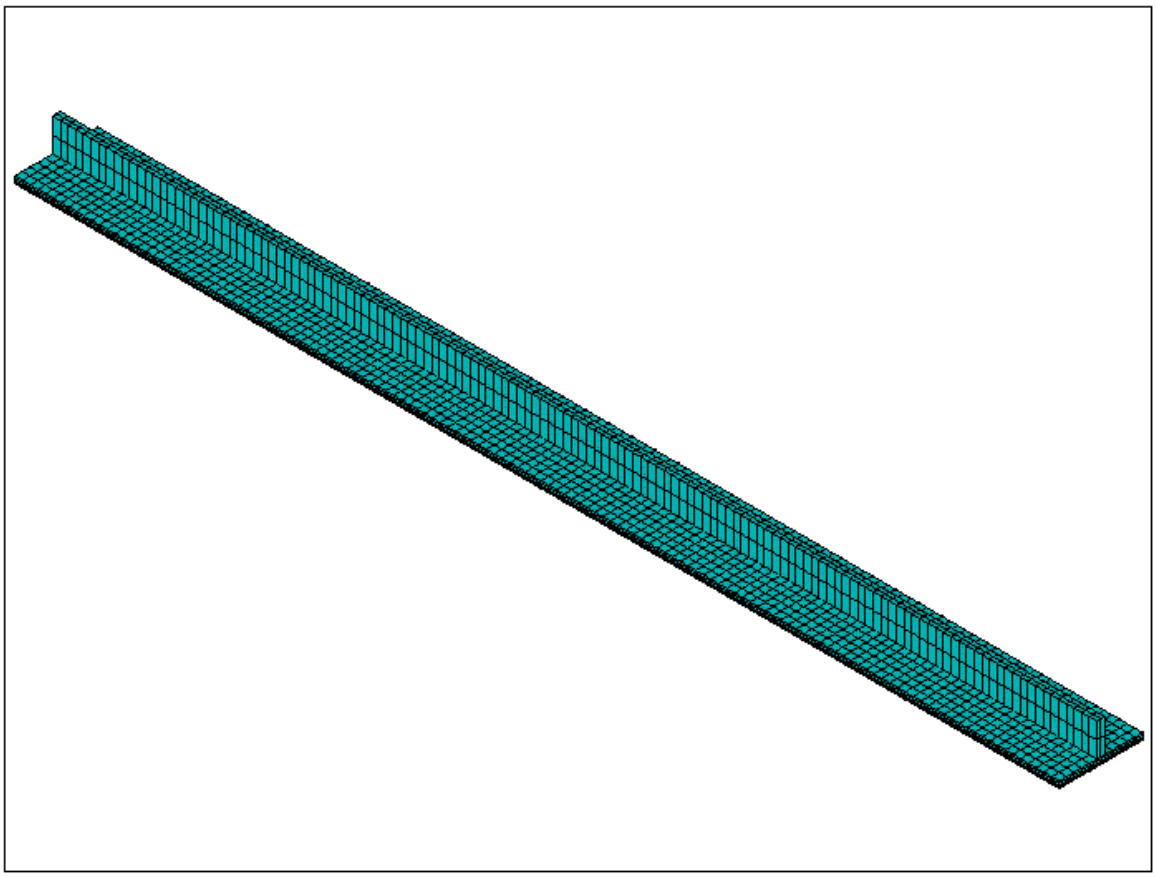

Figure 7.2 FE model of analyzed configuration

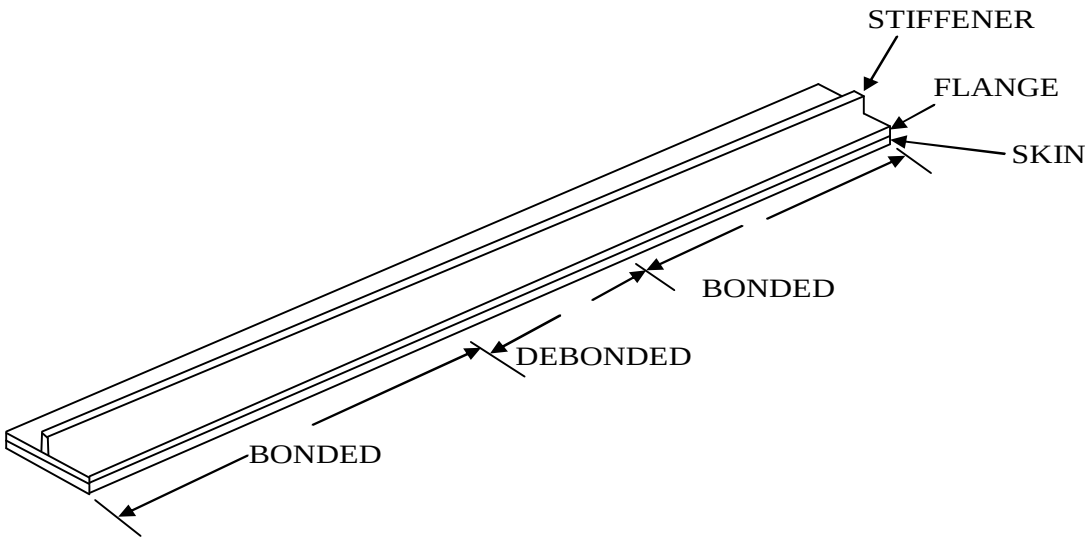

Figure 7.3 Solid model representing initial bonded region

7.3 Numerical results

The numerical compressive load vs. applied displacement curve is represented in Figure 7.4 which shows the global compressive behavior of the panel configuration. The curve obtained by means of proposed numerical methodology (modified subroutine) is compared to the results presented by [82]. An additional analysis has been performed using the standard VCCT-Fail Release approach implemented in the commercial version of the FEM software ANSYS (Ansys Manual). The numerical results in terms of load versus applied displacement curve have been compared with standard VCCT and numerical SMXB-SS results, in figure. It has been found that the result obtained from suggested method has a very good agreement with the existing one. As it can be appreciated in Figure 7.4, the results of all the numerical approaches are almost identical up to the debonding growth initiation. After growth initiation the standard VCCT-based approach tends to overestimate the growth rate leading to a significant reduction in global stiffened panel stiffness.

In nonlinear finite element analyses, strain energy release rates are usually computed for unimodular material properties. While in the preceding analysis, functionally graded bimodular behavior of skin-stiffener has been considered. The objective of this study is to manifest the three dimensional model technique for the investigation of delamination from the initial crack in stiffened panel. Full 3D thermo-elastic finite element analyses have been conducted to account the Strain Energy release rate (SERR) due to the coupled effect of thermo-mechanical and mechanical loading on specimen. The total energy release rate $G_T = G_I + G_{II} + G_{III}$, along the bondline of the specimen is obtained from 3D analysis. The distributions of total mode of strain energy release rate along the delamination front for

different loading conditions and different bimodular ratios on laminated composite have been discussed below.

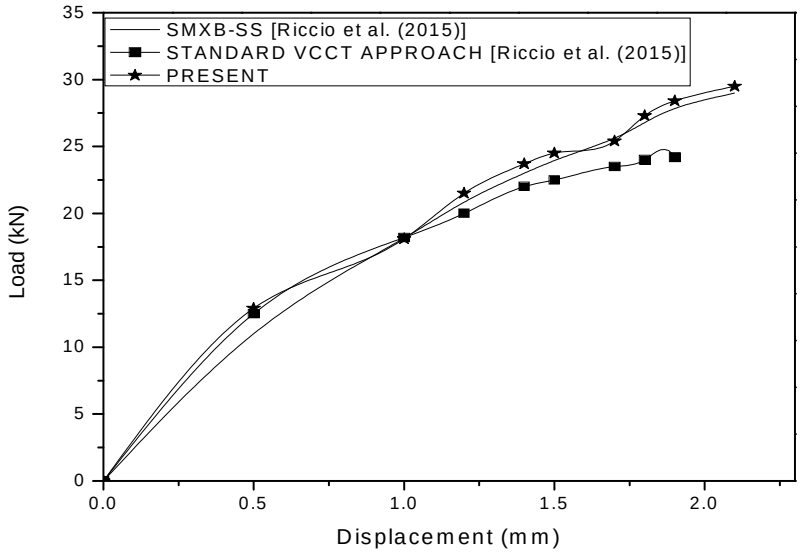

Figure 7.4 Load versus applied displacement curve

7.3.1 Stiffened panel delamination under mechanical loading

The damage of the panel initiates with the failure of the matrix as a consequence of the local instability of the skin flange. Then on increasing the axial load, the fiber failure occurs. The failure analysis indicates that the critical locations for the onset of interfacial failure front. Total mode of SERR, considered as fracture parameters governing the propagation of damages, has been computed along the interfacial failure front. Figure 7.5 exhibits the variation of G_T at the interface of skin and flange with the unimodular material properties (i.e $R=1$) under axial loading. The graph shows the variation under different values of applied load. It is clear from figure that SERR increases with the applied loading value. The debonding starts at the initial value of applied displacement, proceeds to debonding growth initiation and finally damage occurs at applied displacement 2.1mm.

Beyond this, structure collapse and numerical results lose significance and hence not presented.

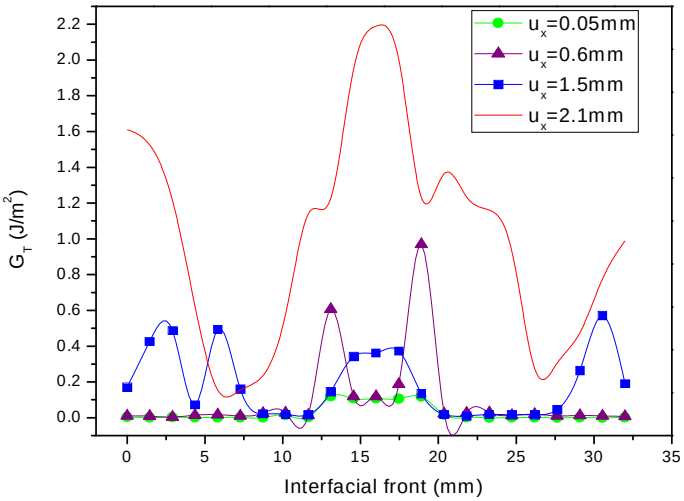

Figure 7.5 Variation of total SERR with varied applied displacement

Strain energy release rate distribution along interfacial front for varied bimodular ratio R under axial loading has been presented in Figure 7.6. The graphs have been drawn for different applied loads. It is significant from the figure that energy release rate attains lower value for large bimodular ratio, which is in good agreement with the results cited in paper [127]. Diagram reveals that G_T is very low and approximately same for R =4 and 5 for all value of u_x. Low energy release rate indicates the retardation of interfacial failure propagation rate of the structure. As the value of compressive load increases, the peak of the graph goes on increasing. It is clear from figure that G attains maximum value in the area of debonding modeled in the skin-stiffener.

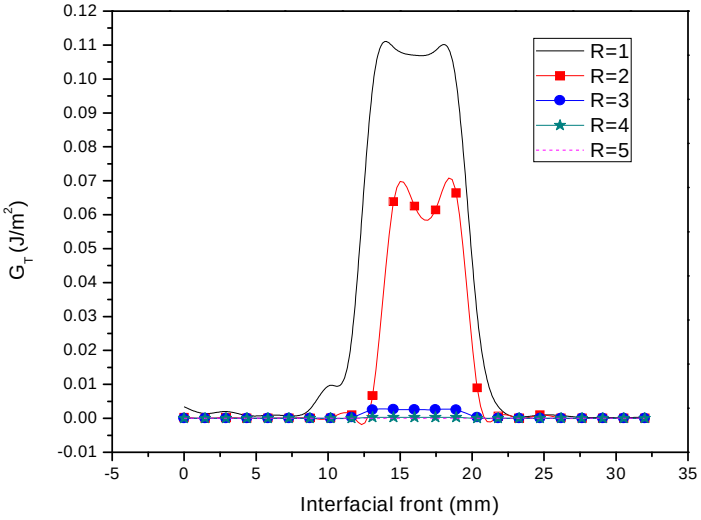
R=1
R=2
R=3
R=4
R=5
G_T (J/m^2)
Interfacial front (mm)

(a)

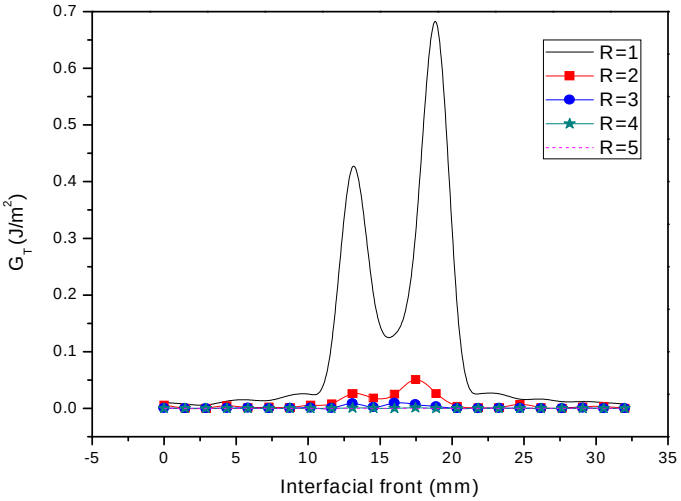
R=1
R=2
R=3
R=4
R=5
G_T (J/m^2)
Interfacial front (mm)

(b)

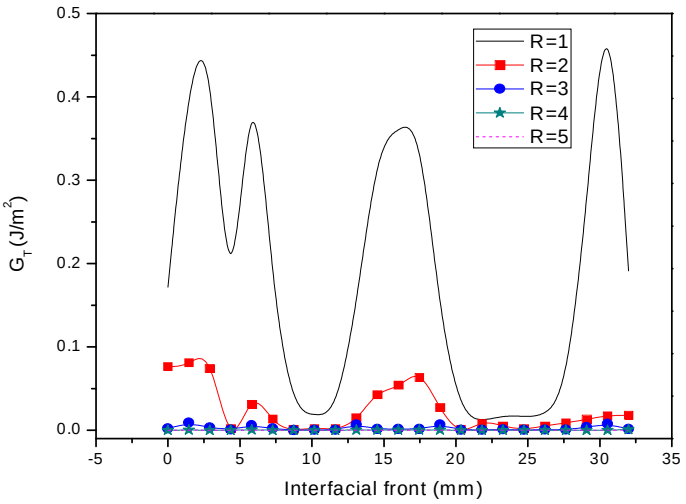

(c)

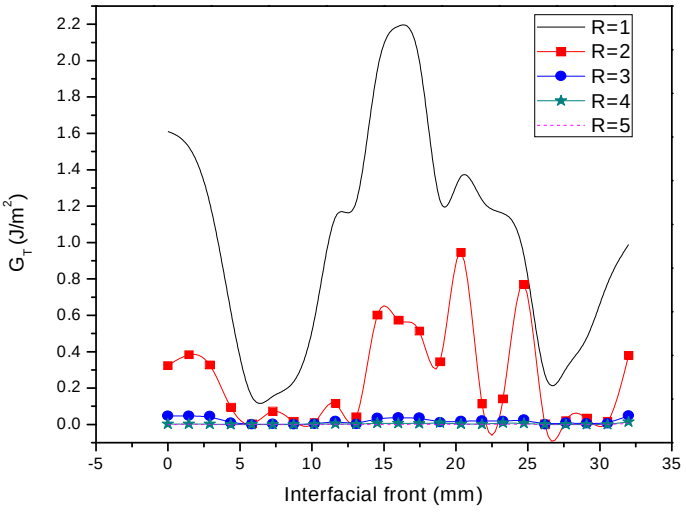

(d)

Figure 7.6 Effect of the applied displacement on total SERR with various bimodular ratio under mechanical loading (a) u_x =0.05mm, (b) u_x =0.6mm, (c) u_x =1.5mm, (d) u_x =2.1mm

7.3.2 Stiffened panel delamination under thermo-mechanical coupled field

The total strain energy release rate has been examined by the numerical technique with modified subroutine for modeled delamination. The SERR along the failure front has been plotted for the debonding between skin and flange under thermal residual stress in Figure 7.7. The pattern of the variation of G_T follows the same configuration as in case of mechanical loading but the energy release rate value is higher in this case. It may be noted that loci of the total SERR (G_T) values are continuously reducing for a varied bimodular material properties of the specimen irrespective of the amount of applied displacement. This indicates that the driving forces are continuously decreasing with respect to bimodular ratio. The behavior of variation of energy release rate in case of coupled field follows the same pattern as the results cited in paper [165]. It is clear that the dominance of failure of structure is when residual thermal stresses have been applied in comparison to the mechanical loading.

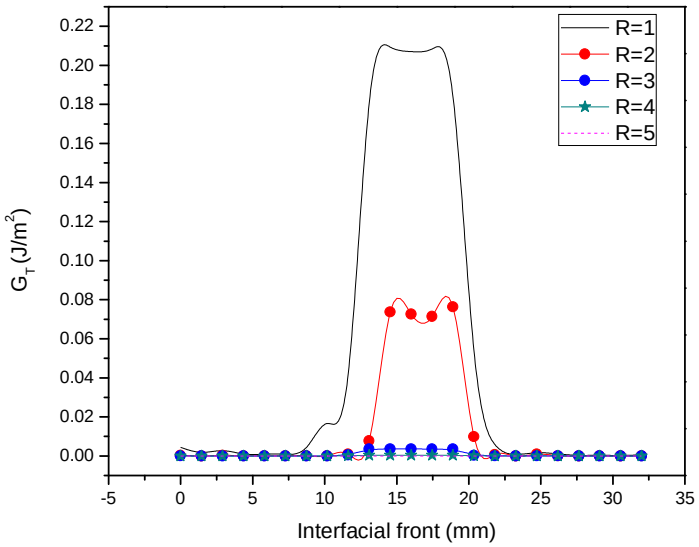

(a)

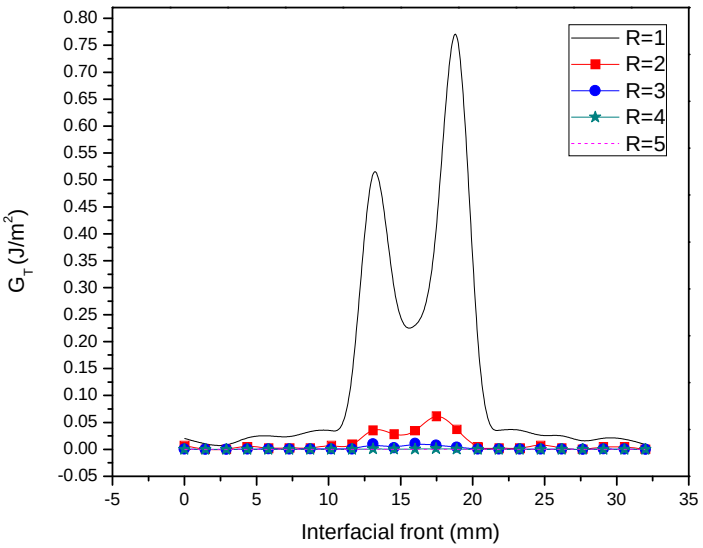
R=1
R=2
R=3
R=4
R=5
G_T (J/m^2)
Interfacial front (mm)

(b)

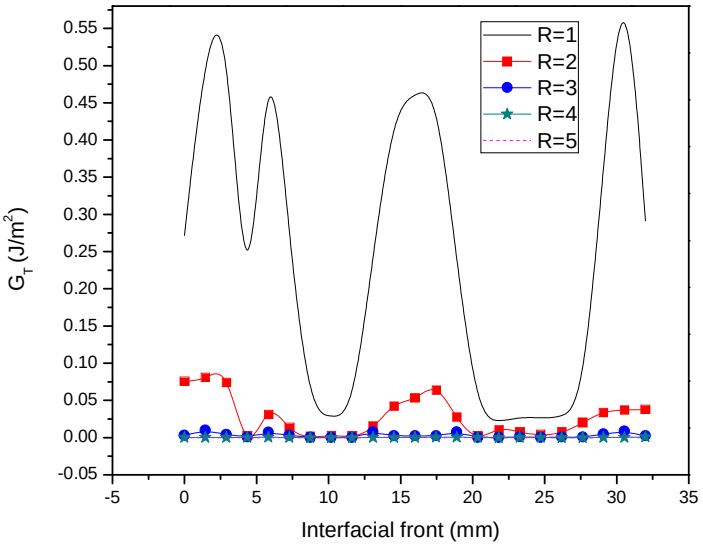
R=1
R=2
R=3
R=4
R=5
G_T (J/m^2)
Interfacial front (mm)

(c)

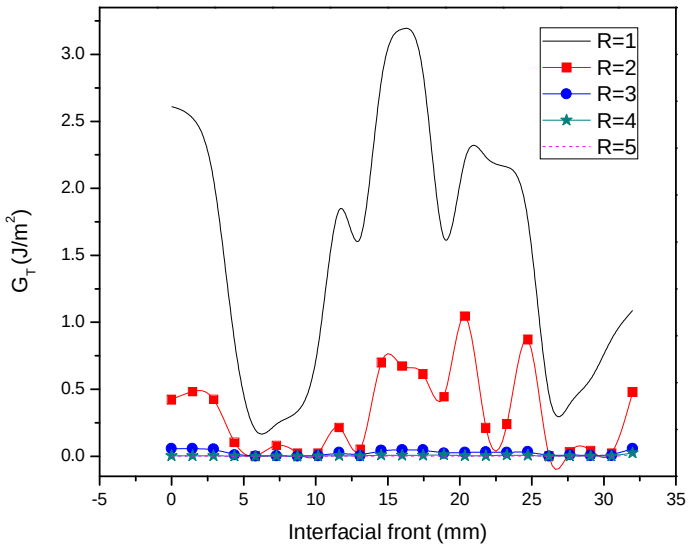

(d)

Figure 7.7 Effect of the applied displacement on total SERR with various bimodular ratio under residual thermal stresses (a) u_x =0.05mm, (b) u_x =0.6mm, (c) u_x =1.5mm, (d) u_x =2.1mm

7.3.3 Comparison of Stiffened panel delamination with and without considering coupled effect of thermal residual stresses and axial loading

In the present work, bimodularity of the skin-stiffener is continuously and smoothly varied along the failure front. In Figure 7.8, the comparison is done for total SERR under mechanical and thermo-mechanical loading for different values of R at the final growth state i.e u_x =2.1mm. It may be concluded from figures that G value is little bit higher in case of coupled field than mechanical loading for all values of R. It is interesting to note that the coupling effect of thermal residual stresses in some cases, enhances the mixed mode interlaminar delamination crack growth, whereas in others, it also opposes the

interface crack growth mechanism depending the location of the delamination front in between skin and flange.

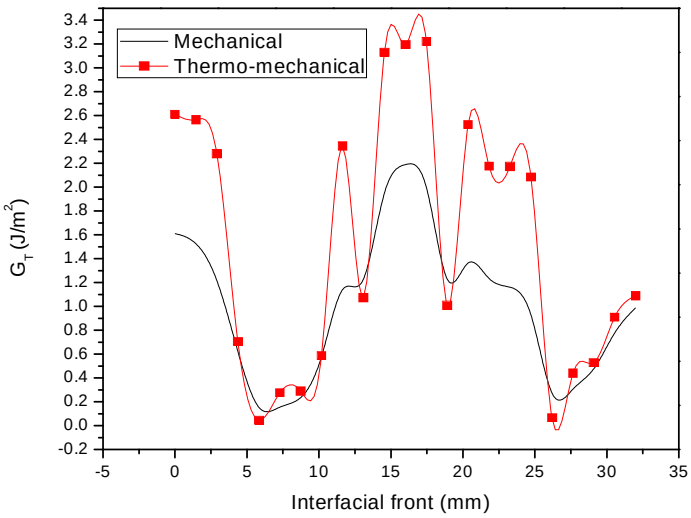

(a)

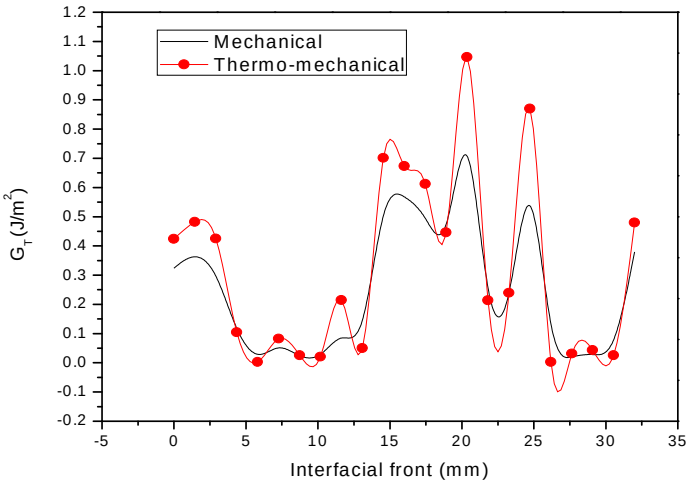

(b)

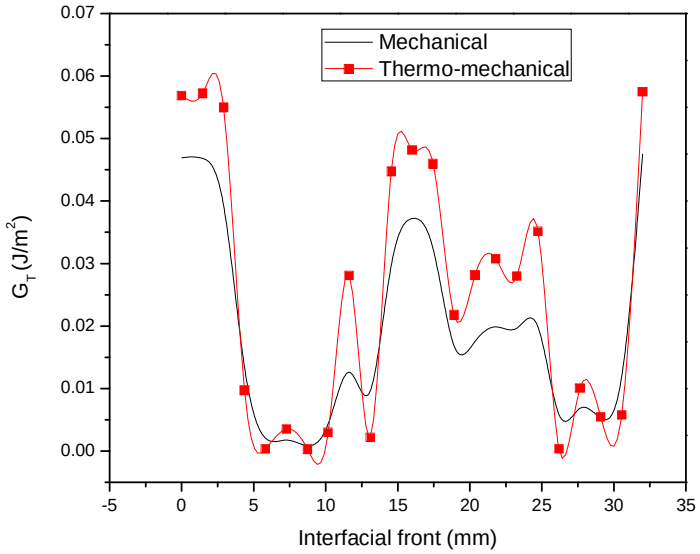
Mechanical
Thermo-mechanical
G_T (J/m^2)
Interfacial front (mm)
0.07
0.06
0.05
0.04
0.03
0.02
0.01
0.00
-5
0
5
10
15
20
25
30
35

(c)

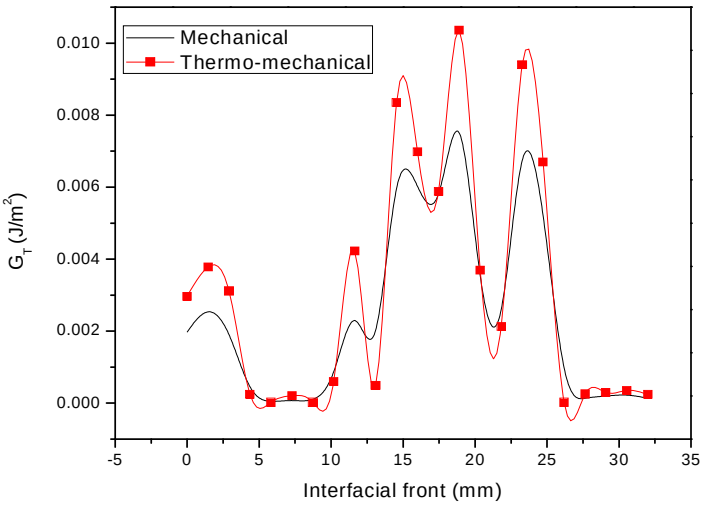
Mechanical
Thermo-mechanical
G_T (J/m^2)
Interfacial front (mm)
0.010
0.008
0.006
0.004
0.002
0.000
-5
0
5
10
15
20
25
30
35

(d)

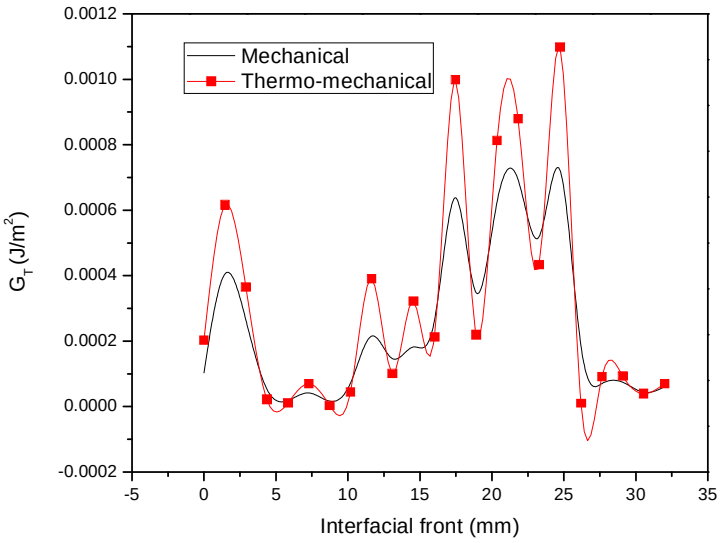

(e)

Figure 7.8 Effect of mechanical and thermo-mechanical loading on total SERR with various bimodular ratio (a) R =1, (b) R =2, (c) R =3, (d) R =4, (e) R =5

7.4 Conclusion

This chapter presents the results of a numerical study on skin-stiffener debonding growth in stiffened composite panel with functionally-grade bimodular material property under residual thermal stresses. A numerical approach with modified subroutine, able to overcome mesh and time step sensitivity problems, has been proposed to investigate the interfacial defects between skin and flange. An excellent agreement of results with previously published data, in terms of load-displacement curve, has been demonstrated. It has been found that strain energy release rate is more when coupled effect of thermal residual stress is considered in comparison to the elastic loading is applied alone. Also, FG bimodularity significantly reduces the damage growth driving force compared to the unimodular material properties but it is significant that bimodular effect is more

pronounced in comparison of functionally graded property. The desirable intention of the skin stiffener designer is to retard interfacial failure propagation rate in order to intensify the structural integrity of the stiffened panel, so that the strength and lifetime of the panel structure can be significantly upgraded. In this paper, efforts have been made to retard the interfacial failure propagation rate by employing functionally-graded bimodular material property.